



Influence of chronic inflammation on the malignant phenotypes and the plasticity of colorectal cancer cells

Sho Watanabe^a, Shuji Hibiya^a, Nobuhiro Katsukura^a, Sayuki Kitagawa^a, Ayako Sato^a,
Ryuichi Okamoto^a, Mamoru Watanabe^{a,b}, Kiichiro Tsuchiya^{a,*}

^a Department of Gastroenterology and Hepatology, Japan

^b Advanced Research Institute, Tokyo Medical and Dental University, Tokyo, Japan

ARTICLE INFO

Keywords:

Sporadic neoplasm
Ulcerative colitis
TP53
Colorectal cancer
Plasticity

ABSTRACT

Sporadic adenoma or adenocarcinoma is often detected during endoscopic surveillance of patients with ulcerative colitis (UC). However, it is occasionally difficult to distinguish these neoplasms from dysplasia or colitis-associated cancers because of the influence of inflammation. However, the influence of inflammation on sporadic neoplasms is not well characterised. To assess this influence, we established a long-term inflammation model of colon cancer cells by inflammatory stimulation with tumour necrosis factor- α , flagellin and interleukin-1 β for 60 weeks. Then, the malignant phenotypes were evaluated using the MTS assay, Annexin V fluorescence assay, cell migration assay and sphere formation assay. The influence of P53 function on these phenotypes was assessed with a TP53 mutation model using the CRISPR/Cas9 system. A long-term inflammation model of LS174T cells was established for the first time with continuous inflammatory signalling. Chronic inflammation induced apoptosis and suppressed the proliferation and stemness of these cancer cells via the action of P53. It also enhanced the invasiveness of LS174T cells. Moreover, these phenotypic changes and changes in inflammatory signalling were recoverable after the removal of inflammatory stimuli, suggesting that colon cancer cells have higher plasticity than normal intestinal epithelial cells. In conclusion, our results suggest that sporadic neoplasms in patients with UC are affected by chronic inflammation but are not essentially altered.

1. Introduction

Ulcerative colitis (UC) is a type of chronic inflammatory bowel disease involving the colon and is characterised by frequent relapse. Long-standing UC is a known risk factor for dysplasia or colitis-associated cancer (CAC) [1], the carcinogenic process of which is referred to as dysplasia–carcinoma sequence based on *TP53* mutation [2]. On the other hand, the carcinogenic process of sporadic adenoma or adenocarcinoma is referred to as adenoma–carcinoma sequence based on *APC* mutation [3], which is also detected during endoscopic surveillance of UC [4]. Because sporadic neoplasms in UC are reported to show better prognosis than CAC, accurate diagnosis is very important. The differential diagnosis of these tumours is usually based on endoscopic findings, pathological characteristics and immunohistochemical staining for P53 and Ki-67 [4,5]. However, it is sometimes difficult to distinguish

these tumours [4]. One of the reasons is that not only CAC but also sporadic neoplasms may be affected by chronic inflammation. However, the influence of chronic inflammation on sporadic neoplasms are not well characterised. In other words, it is unclear whether the phenotypes of sporadic adenoma or adenocarcinoma cells are affected by chronic inflammation. We previously established a human UC organoids model using inflammatory reagents *in vitro*, in which chronic inflammation induced irreversible changes in the inflammatory signals and phenotypes (cell proliferation, apoptosis, stemness and histological changes) of human colon organoids [6]. We also reported that *TP53* mutation using the lentiviral CRISPR/Cas9 system enhanced malignant phenotypes (cell proliferation, invasiveness, cancer stemness and chemoresistance) of LS174T cells [7] with wild-type *TP53*. For the above reasons, we hypothesised that the malignant phenotypes of colorectal cancer cells would also be altered by chronic inflammation. In the

Abbreviations: colitis-associated cancer, CAC; wild-type TP53, TP53WT; extreme limiting dilution analysis, ELDA; zinc transcription factor, ZEB1; epithelial–mesenchymal transition, EMT; leucine-rich repeat-containing G-protein-coupled receptor 5, Lgr5.

* Corresponding author. Department of Gastroenterology and Hepatology, Graduate School, Tokyo Medical and Dental University, 1-5-45 Yushima, Bunkyo-ku, Tokyo, 113-8519, Japan.

E-mail address: kii.gast@tmd.ac.jp (K. Tsuchiya).

<https://doi.org/10.1016/j.bbrep.2021.101031>

Received 7 April 2021; Received in revised form 13 May 2021; Accepted 17 May 2021

2405-5808/© 2021 Published by Elsevier B.V. This is an open access article under the CC BY-NC-ND license (<http://creativecommons.org/licenses/by-nc-nd/4.0/>).

present study, a long-term inflammation model of a colorectal cancer cell line (LS174T cells) was established for the first time. This model revealed that the malignant phenotypes of LS174T cells were altered under chronic inflammation: the suppression of cell proliferation and cancer stemness due to apoptosis via P53 action and the enhancement of invasiveness. Moreover, these phenotypic changes were recoverable after the cessation of chronic inflammation, suggesting that colon cancer cells have higher plasticity than normal intestinal epithelial cells (IECs).

2. Materials and methods

2.1. Study approval

The study protocol was approved by the Ethics Committee of the Tokyo Medical and Dental University (Tokyo, Japan).

2.2. Cell culture and chemicals

The human colon adenocarcinoma-derived cell line LS174T, which expresses wild-type TP53 (TP53WT), was cultured in Dulbecco's modified Eagle's medium (Life Technologies, Grand Island, NY, USA) supplemented with 10% fetal bovine serum and 1% penicillin/streptomycin as previously described [8,9]. In addition, 100 ng/mL of flagellin (Invitrogen Corporation, Carlsbad, CA, USA), 10 ng/mL of human interleukin (IL)-1 β (PeproTech, Rocky Hill, NJ, USA) and 100 ng/mL of human tumour necrosis factor (TNF)- α (PeproTech) reagents were added to the media at the passage individually or in combination (once per week). LS174T cells with or without inflammatory stimulation were simultaneously cultured for the same period.

2.3. CRISPR/Cas9-mediated mutagenesis of TP53

The mutation of exon 10 of TP53 in LS174T cells was performed with the CRISPR/Cas9 system using lentivirus as previously described [7]. The target array sequence is summarised in [Supplementary Table 1](#). After puromycin and P53 functional selection with Nutlin3a for 1 week, dissociated single cells were cultured and the deletion of eight bases in the TP53 exon 10 was confirmed [7]; the resulting LS174T cells had the shorter form of P53 protein (377 amino acids), with a mutation at the tetramerisation domain [7]. These TP53-mutated LS174T cells acquired more malignant phenotypes and showed lower expression of P53 downstream genes such as P21 and PUMA [7].

2.4. Quantitative real-time polymerase chain reaction (PCR) analysis

Total RNA was isolated using a RNeasy Micro Kit (Qiagen, Hilden, Germany). Aliquots of 1 μ g of total RNA were used for complementary DNA (cDNA) synthesis. cDNA synthesis and real-time PCR were performed as previously described [10]. The primer sequences are presented in [Supplementary Table 1](#). β -ACTIN was employed as an endogenous housekeeping gene. Delta CT values were calculated in relation to β -ACTIN CT values using the $2^{-\Delta\Delta CT}$ method as previously described [8].

2.5. Immunofluorescence analysis

Immunofluorescence analysis was performed as previously described [11,12]. The cells were fixed as previously described [13] and labelled with antibodies specific for P65 (2118S, CST). Anti-rabbit IgG Alexa Fluor[®] 488 (Invitrogen) was used as the secondary antibody. The stained cells were mounted with VectaShield mounting medium containing 4',6-diamidino-2-phenylindole (Vector Laboratories, Burlingame, CA, USA) and visualised using a confocal laser fluorescent microscope (BZ-X700; Keyence, Tokyo, Japan and FLUOVIEW FV10i; Olympus, Tokyo, Japan). Nuclear translocation of NF- κ B p65 was quantified as the ratio of the fluorescence intensity in the nuclei to that

in the cytoplasm in 30 cells per well using ImageJ software (National Institutes of Health, Bethesda, MD, USA; <http://imagej.nih.gov/ij/>) as previously described [6].

2.6. MTS assay

Cell proliferation was evaluated using the MTS assay as previously described [7,12]. Cells were cultured in 96-well tissue culture plates at a density of 1×10^4 cells per well. After incubation for 24 or 96 h, Cell Titer 96[®] Aqueous One Solution (20 μ L/well; Promega, Madison, WI, USA) was added, and the cells were incubated again for 1 h at 37 $^{\circ}$ C in 5% CO₂. In each well, the absorbance at 490 nm was measured using a Glomax[®] Discover Microplate Reader (Promega). Background absorbance in wells containing medium alone was subtracted from that of the sample wells. The cell proliferation ratio was calculated as the ratio of absorbance at 96 h to that at 24 h.

2.7. Cell cycle analysis

The cell cycle was assessed using the BD FACS Canto II (BD bioscience) with a violet 405 nm laser diode as previously described [6,14]. Dissociated cells were filtered with a 20- μ m cell strainer. Cells were incubated with 10 μ g/mL Hoechst 33342 (1:1000, Lonza) for 20 min at room temperature. After gating on single cells, cells were gated using width and area parameters from Hoechst 33342. The area parameter histogram was used to determine the percentage of cells in the G1, S and G2M phases according to the manufacturer's protocol.

2.8. Annexin V fluorescence analysis

Apoptosis was evaluated using Annexin V fluorescence analysis as previously described [7,15]. Cells were cultured in a 12-well plate at a density of 1×10^4 cells per well. After incubation for 96 h, Annexin V-Alexa Fluor[™]594 conjugate (Invitrogen) and Hoechst 33342 (1:1000, Lonza) were added according to the manufacturer's instructions. The cells were visualised using a confocal laser fluorescent microscope (BZ-X700; Keyence and FLUOVIEW FV10i; Olympus). ImageJ software was used to assess the fluorescence intensity of 30 cells per group.

2.9. Migration assay

The invasiveness of LS174T cells was evaluated using the migration assay as previously described [7,12]. The Oris Pro Cell Migration Assay kit (Platypus Technologies, Madison, WI, USA) was used according to the manufacturer's protocol. This assay is formatted for 96-well plates and employs a nontoxic biocompatible gel to form a cell-free zone on the cell culture surface. A total of 2×10^4 cells were seeded into each well and incubated for 1 h. Pre-migration phase-contrast images were obtained for reference. After incubation for 12 h, additional phase-contrast images were captured. The ratio of the vacant area in pre- and post-migration images was then analysed.

2.10. In vitro sphere formation assay

The cancer stemness of LS174T cells was evaluated using the *in vitro* sphere formation assay as previously described [7,12]. LS174T cells were cultured at various densities (1000, 500, 250 and 125 cells/well) in Matrigel[®] GFR (Corning, Corning, NY, USA) with stem cell medium (SCM) in a 24-well tissue culture plate. SCM was prepared using the following reagents: 500 mL of 1:1 ratio of DMEM/F12 (Invitrogen), 1% penicillin/streptomycin, B27 supplement (Invitrogen), 4 μ g/mL heparin, 1% (w/v) nonessential amino acids, 1% (w/v) sodium pyruvate, 1% (w/v) L-glutamine, 10 ng/mL fibroblast growth factor and 20 ng/mL epidermal growth factor. After culturing for 7 days, the number of spheroids was counted. The spheroid formation ability was calculated using a software application for extreme limiting dilution analysis

(ELDA), as described previously [7].

2.11. Statistical analysis

Prism software (GraphPad Software, San Diego, CA, USA) was employed to calculate standard deviations (SD) and the statistical significance of differences between samples. All results were represented as the mean \pm SD. Two-sided Student's or paired *t*-test was used for statistical analysis. P values < 0.05 were considered indicative of statistical significance.

3. Results

3.1. Establishment of the LS174T cell model with long-term inflammation

To mimic the clinical history of UC, an *in vitro* chronic inflammation model was established with LS174T cells based on the methods described in our previous reports [6,16]. First, we assessed the induction of *IL-8* expression after treatment with inflammatory reagents. LS174T

cells treated with a mixture of inflammatory reagents showed higher induction of *IL-8* than cells subjected to individual treatments (Fig. 1A); this suggested that the mixture was sufficient for the establishment of a chronic inflammation model similar to the previous organoids model [6]. LS174T cells treated with this mixture were steadily maintained for 60 weeks, similar to the cells without inflammatory stimulation [Inf(-) cells] (Fig. 1B). The expression of *IL-8* was continuously induced during the 60-week stimulation period (Fig. 1C). Continuous nuclear accumulation of NF- κ B p65 in the inflamed LS174T cells indicated the successful generation of LS174T cells with long-term inflammation [Inf(+)] cells (Fig. 1D and E).

3.2. Inflammatory response of inflamed LS174T cells was restored to the normal level after removal of inflammatory stimuli

According to our UC-mimicking model using human colon organoids [6], inflammatory reagents were removed from the culture medium of the long-term inflamed cells to assess the reversibility of the effects of long-term inflammation on LS174T cells (Fig. 2A). Unlike that in the

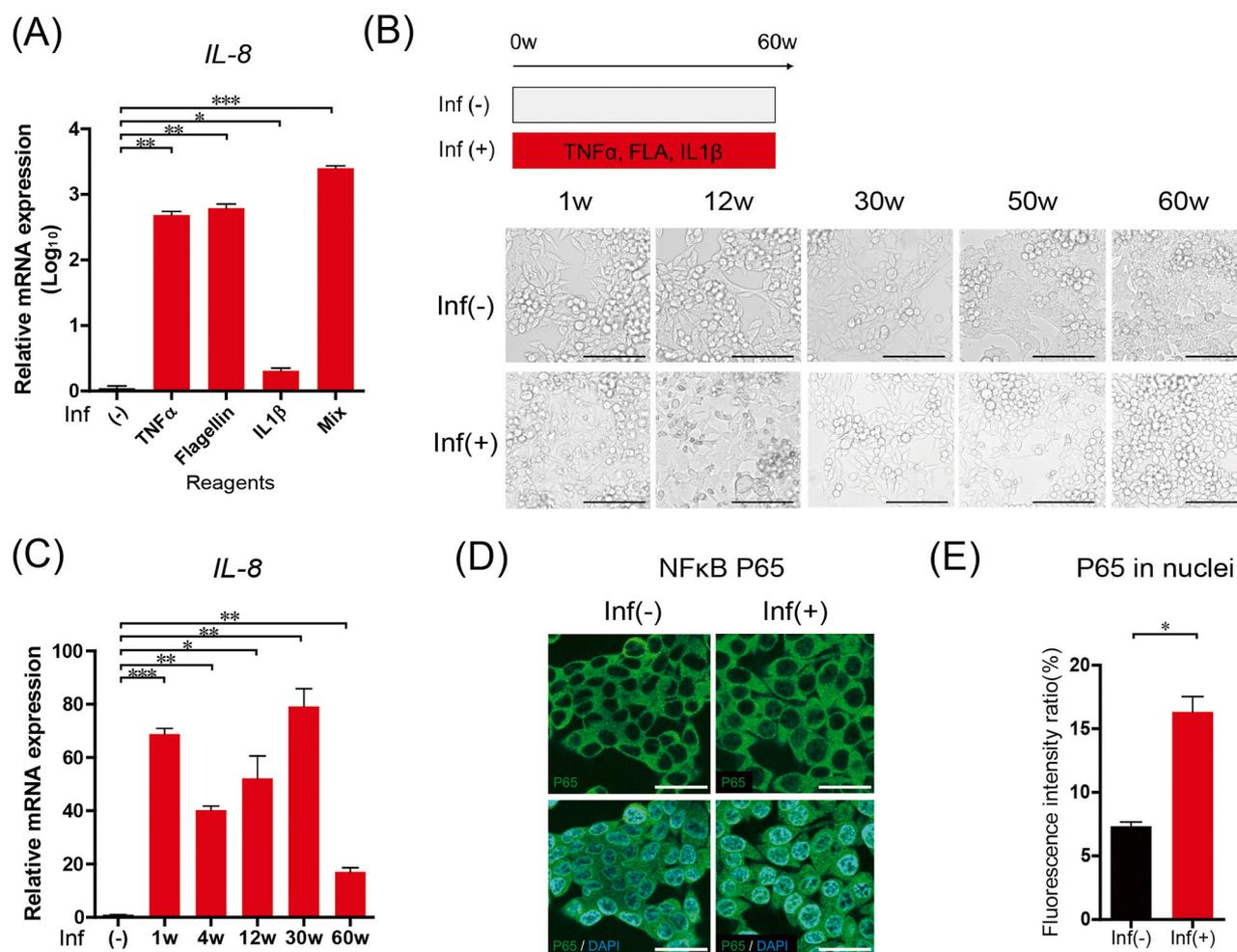


Fig. 1. Establishment of the LS174T cell model with long-term inflammation. (A) Expression of *IL-8* was assessed using RT-PCR. Treatment of LS174T cells with TNF- α , flagellin (FLA), and IL-1 β for 3 h resulted in significant induction of *IL-8* expression. A mixture of these inflammatory reagents induced higher induction of *IL-8* than individual treatments. (B) A schema of long-term inflammatory stimulation of LS174T cells (upper panel). A series of representative pictures of LS174T cells treated with or without mixed inflammatory reagents during continuous culture for 60 weeks (lower panel). Abbreviations: Inf(-) or Inf(+): LS174T cells cultured for 60 weeks without or with mixed inflammatory reagents, respectively. Scale bar: 100 μ m. (C) Results of RT-PCR showing chronological changes in the expression of *IL-8* (NF- κ B downstream gene) in LS174T cells with inflammatory stimulation for 1–60 weeks. (D) Immunofluorescence of p65 in LS174T cells. The localisation of p65 was shifted to the nuclei of LS174T cells after inflammatory stimulation for 60 weeks. Scale bar: 25 μ m. (E) Quantification of the nuclear translocation of NF- κ B p65. Nuclear translocation of p65 was significantly promoted by long-term inflammation; 30 cells were assessed per well. (A, C, E) The result is from single experiment using three replicate wells. (D, E) Two independent experiments were conducted. Results are presented as mean \pm standard deviation; (A, E) two-sided Student's *t*-test and (C) two-sided paired *t*-test. (A–E) **p* < 0.05, ***p* < 0.01, ****p* < 0.001.

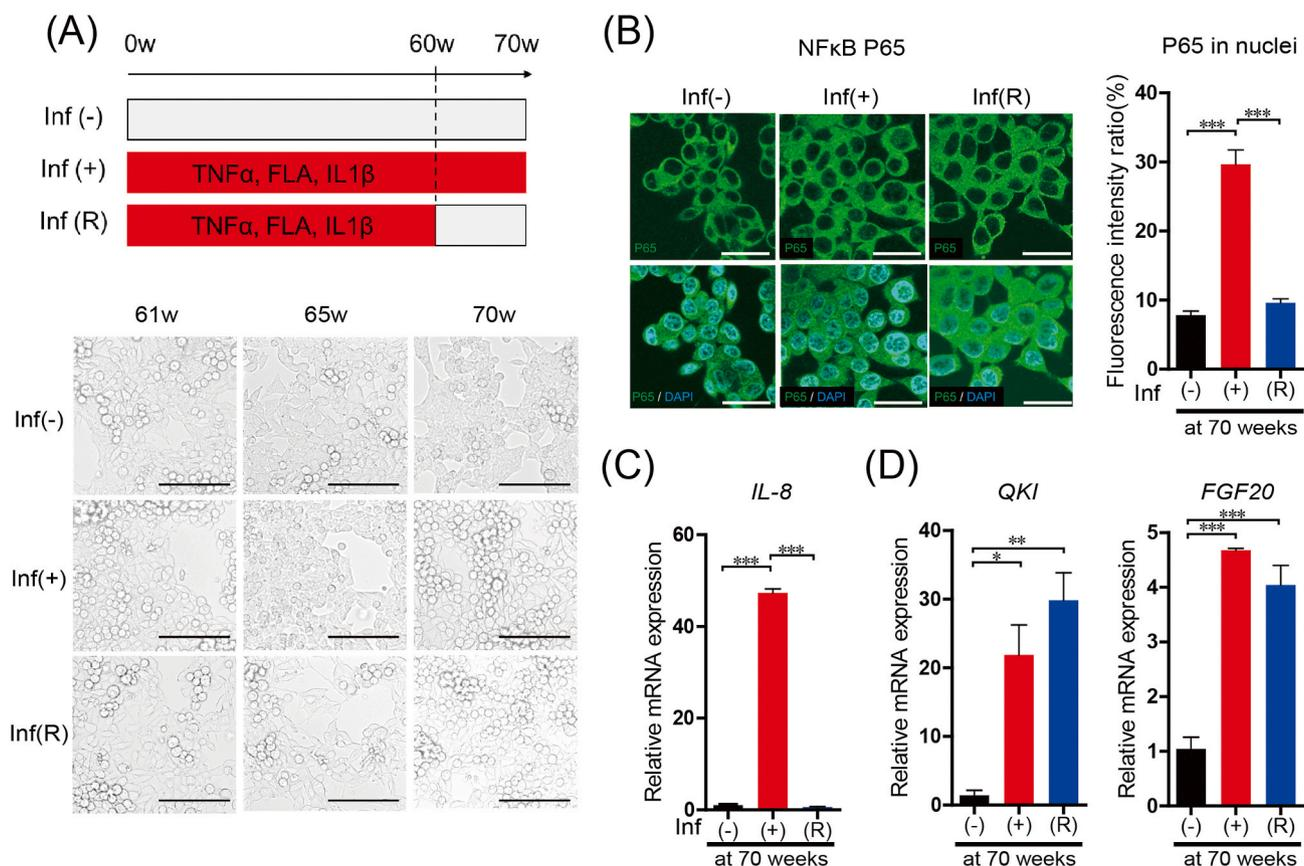


Fig. 2. Inflammatory response of LS174T cells induced by long-term inflammation is recoverable after the removal of inflammatory stimuli. (A) A schema of the establishment of inflammation-removed LS174T cells (upper panel). Abbreviations: Inf(R) cells: LS174T cells 10 weeks after the removal of 60-week inflammatory stimulation. A series of representative pictures of Inf(R) and control [Inf(-) and Inf(+)] cells from 61 to 70 weeks (lower panel). Scale bar: 100 μ m. (B) Immunofluorescence and quantification of the nuclear translocation of NF- κ B p65. Nuclear translocation of p65 induced by 60-week inflammation was restored to the normal level; 30 cells were assessed per well. Scale bar: 25 μ m. (C) Results of RT-PCR showing the expression levels of NF- κ B-related genes. *IL-8* expression induced with 60-week inflammation was recovered to the normal level after the removal of inflammatory stimuli. (D) Results of RT-PCR showing the expression levels of chronic inflammation-specific marker genes identified in our previous UC-mimicking model [6]. Induction of *QKI* and *FGF20* expression by 60-week inflammation was not recoverable after the removal of inflammatory stimuli. (B–D) The result is from single experiment using three replicate wells. (B–D) Two independent experiments were conducted. Results are presented as mean \pm standard deviation; (B–D) two-sided Student's *t*-test. (B–D) **p* < 0.05, ***p* < 0.01, ****p* < 0.001.

UC-mimicking model [6], NF- κ B signalling of LS174T cells induced by chronic inflammation was restored to the normal level 10 weeks after the removal of inflammatory stimuli [Inf(R) cells] (Fig. 2B and C), although long-term inflammation-specific genes (*QKI* and *FGF20*), which were extracted in our UC-mimicking organoids model [6], were also irreversibly induced in long-term inflamed LS174T cells (Fig. 2D).

3.2.1. Cancer cell proliferation and viability are suppressed by chronic inflammation via the action of P53 but are restored to normal levels after the removal of inflammatory stimuli

We subsequently assessed the effects of chronic inflammation on the malignant phenotype of LS174T cells. The cell proliferation ratio of LS174T cells was suppressed by chronic inflammation but was restored to normal levels after the removal of inflammatory stimuli (Fig. 3A). The proportion of cells at the G2M phase and *c-myc* expression were also suppressed by chronic inflammation but were restored to normal levels after the removal of inflammatory stimuli (Fig. 3B and C). On the other hand, Annexin V fluorescence and *PUMA* expression showed that chronic inflammation induced apoptosis of LS174T cells (Fig. 3D and E). Annexin V fluorescence was restored to the normal level after the removal of inflammatory stimuli (Fig. 3D), although *PUMA* expression was still induced (Fig. 3E). Collectively, these results suggest that the proliferation and viability of LS174T cells were suppressed by chronic inflammation but were restored to normal levels after the removal of inflammatory stimuli. To assess the influence of P53 function on these

phenotypic changes by chronic inflammation, we established a long-term inflammation model of TP53-mutated LS174T cells (Supplementary Fig. 1A). The TP53-mutated cells under chronic inflammation also exhibited enhancement of NF- κ B signalling (Supplementary Fig. 1B, C). Subsequently, the proliferation and viability of TP53-mutated cells under chronic inflammation were compared with those of TP53WT cells. TP53-mutated cells had a higher cell proliferation ratio under inflammation than TP53WT cells (Supplementary Fig. 1D). The proportion of TP53-mutated cells at the G2M phase was higher than that of TP53WT cells under chronic inflammation (Supplementary Fig. 1E). *P21* expression under chronic inflammation was suppressed in TP53-mutated cells (Supplementary Fig. 1F). On the other hand, *PUMA* expression and Annexin V fluorescence showed suppression of apoptosis in TP53-mutated cells under chronic inflammation (Supplementary Fig. 1G, H). Collectively, these findings suggest that TP53-mutated cells show higher proliferation and viability under chronic inflammation and that these phenotypic changes by chronic inflammation are mediated by P53 function.

3.2.2. Invasiveness and cancer stemness are altered by chronic inflammation but are restored to normal levels after the removal of inflammatory stimuli

Chronic inflammation promoted migration of LS174T cells (Fig. 4A). Additionally, chronic inflammation also induced the expression of human zinc transcription factor (*ZEB1*), which is a key regulator of

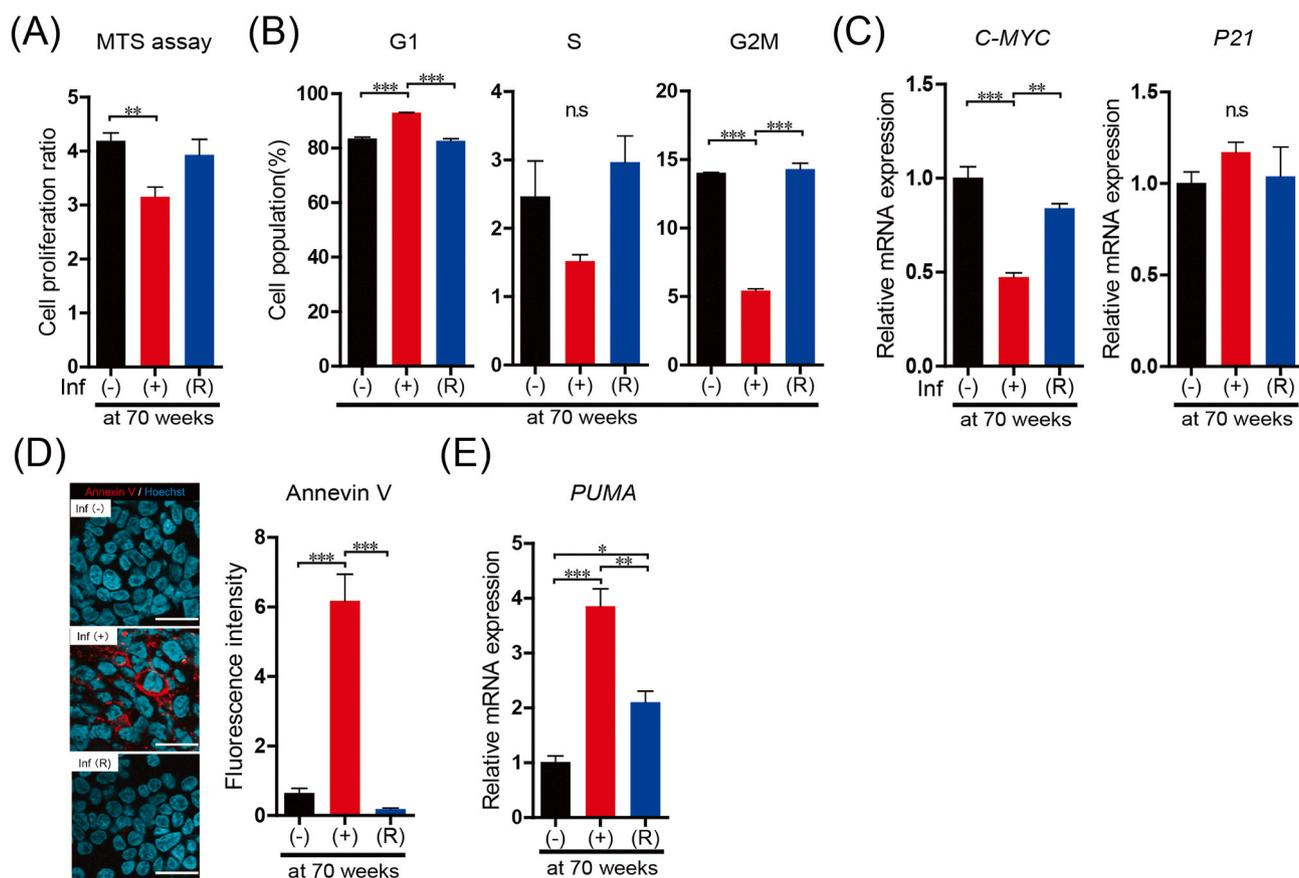


Fig. 3. Proliferation and viability of LS174T cells were suppressed by chronic inflammation but were recoverable after the removal of inflammatory stimuli. (A) Results of MTS assay showing the cell proliferation ratio. Cell proliferation was significantly suppressed by chronic inflammation but was restored after the removal of inflammatory stimuli. (B) Cell cycle assay of LS174T cells with Hoechst 33342. The area parameter histogram was used to determine the percentage of cells in the G1, S and G2M phases. Inf(+) cells showed a higher proportion in the G1 phase and lower proportion in the G2M phase, but Inf(-) cells showed a similar proportion as Inf(-) cells in each phase. (C) Analysis of cell cycle progression genes using RT-PCR. *C-MYC* expression was suppressed by chronic inflammation, although it was restored to the normal level after the removal of inflammatory stimuli. *P21* expression was not altered by chronic inflammation. (D) The state of apoptosis in each group was evaluated using Annexin V-Alexa Fluor™594 conjugate (left panel). The fluorescence intensity of Annexin V was calculated in 30 cells per well. Apoptosis was induced by chronic inflammation [Inf(+) cells] but was suppressed to normal levels after the removal of inflammatory stimuli [Inf(R) cells] (right panel). Scale bar: 25 μ m. (E) Analysis of the expression levels of apoptosis-related genes using RT-PCR. *PUMA* expression was induced by chronic inflammation. The expression was still induced after the removal of chronic inflammatory stimuli. The result is from single experiment using (A) five or (B–E) three replicate wells. (A, C–E) Two independent experiments were conducted. Results are presented as mean \pm standard deviation; (A–E) two-sided Student's *t*-test. (A–E) **p* < 0.05, ***p* < 0.01, ****p* < 0.001.

transforming growth factor- β -induced epithelial–mesenchymal transition (EMT) [17] (Fig. 4B); this suggested that chronic inflammation promoted the invasiveness of LS174T cells. However, the invasiveness of LS174T cells was restored to normal levels after the removal of inflammatory stimuli (Fig. 4A and B). Chronic inflammation suppressed sphere formation of LS174T cells (Fig. 4C) and also suppressed the expression of *leucine-rich repeat-containing G-protein-coupled receptor 5* (*Lgr5*), which is a known cancer stem cell marker [18] (Fig. 4D); this suggested that chronic inflammation suppressed the cancer stemness of LS174T cells. However, the cancer stemness of LS174T cells was restored to normal levels after the removal of inflammatory stimuli (Fig. 4C and D). We then assessed the influence of P53 function on these phenotypes under chronic inflammation. Interestingly, migration under chronic inflammation was further promoted in TP53-mutated cells (Supplementary Fig. 2A). Moreover, *ZEB1* expression was also further induced by TP53 mutation under inflammation (Supplementary Fig. 2B). TP53-mutated cells showed a higher degree of sphere formation under inflammation than TP53WT cells (Supplementary Fig. 2C). *Lgr5* expression was also higher in TP53-mutated cells than in TP53WT cells (Supplementary Fig. 2D), suggesting that TP53-mutated cells had higher cancer stemness than TP53WT cells under chronic inflammation.

4. Discussion

Recent studies have elucidated the pathogenesis and characteristics of CAC. Several studies have also reported differences in the characteristics and prognosis between CAC and sporadic colorectal cancer in patients without UC. However, the characteristics of sporadic neoplasm in patients with UC are not well characterised. In this study, we established a LS174T chronic inflammation model to evaluate the influence of chronic inflammation on sporadic neoplasm. This model showed continuous induction of inflammatory signals in colorectal cancer cells, similar to that in normal human colon organoids [6]. In addition, proliferation of cancer cells was suppressed by chronic inflammation through the suppression of cell cycle and the promotion of apoptosis, similar to that in normal human colon organoids [6]. These results suggest that the tolerance to chronic inflammation, including apoptosis, was not induced even in colorectal cancer cells. Interestingly, chronic inflammation significantly promoted cell migration and *ZEB1* expression. In a previous study, inflammation was shown to induce *ZEB1* expression, which in turn promoted EMT [19]. Therefore, our data suggest that chronic inflammation enhances the invasiveness of colorectal cancer cells.

To assess the influence of P53 function on sporadic neoplasm under

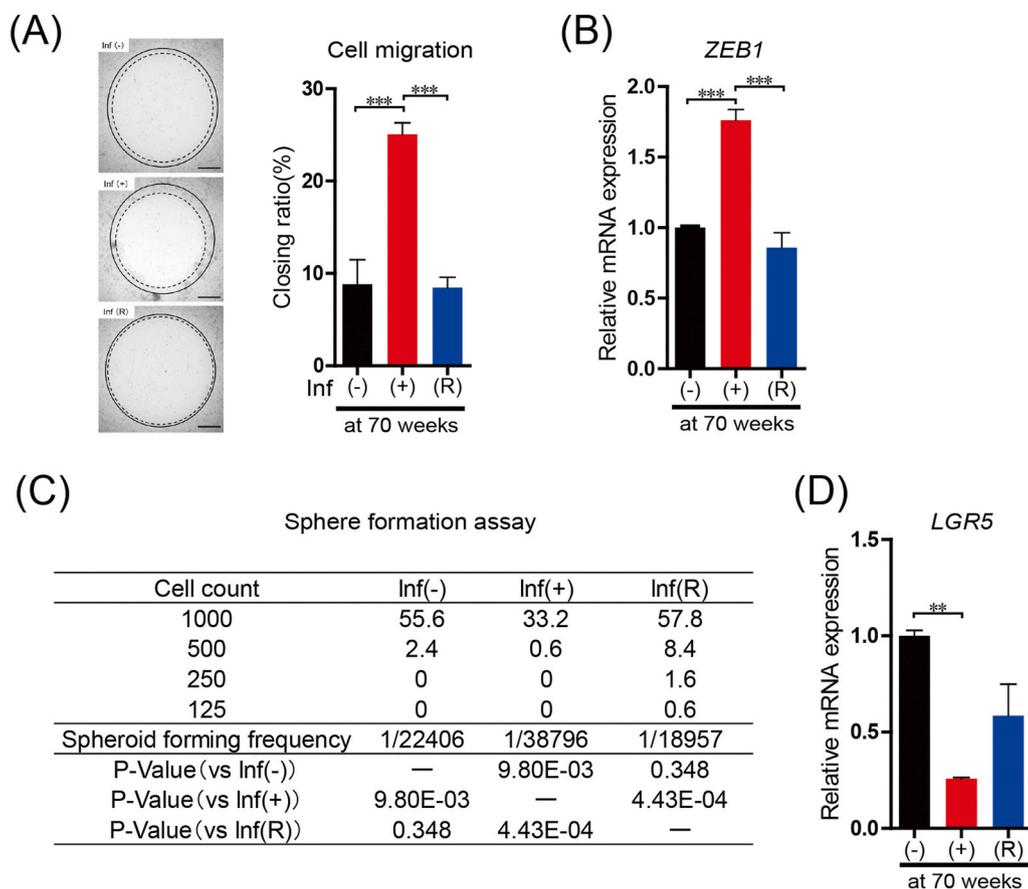


Fig. 4. Invasiveness and stemness of LS174T cells were altered by chronic inflammation but were recoverable after the removal of inflammatory stimuli. (A) The migration assay revealed that chronic inflammation promoted the migration of LS174T cells to the vacant area. The solid line and the dashed line in each figure show the borderline of LS174T cells at 30 min and 12 h after seeding, respectively (left panel). The closing ratios of the remaining vacant areas are shown (at 12 h/at 30 min). The closing ratio of LS174T cells was promoted by chronic inflammation, although it was restored to the normal level after the removal of inflammatory stimuli (right panel). Scale bar, 500 μ m. (B) Analysis of the expression levels of cancer invasiveness-related genes using RT-PCR. *ZEB1* expression was induced by chronic inflammation, although it was restored to the normal level after the removal of inflammatory stimuli. (C) Results of the sphere formation assay analysed with ELDA methods. The sphere forming frequency was significantly suppressed by chronic inflammation but was restored by the removal of inflammatory stimuli. (D) Analysis of the expression levels of stem cell marker genes using RT-PCR. *LGR5* expression was suppressed by chronic inflammation, although it was restored to the normal level after the removal of inflammatory stimuli. The result is from single experiment using (A) six or (B–D) three replicate wells. (A–D) Two independent experiments were conducted. Results are presented

as mean \pm standard deviation; (A–D) two-sided Student's *t*-test. (A–D) ***p* < 0.01, ****p* < 0.001.

chronic inflammation, we established a chronic inflammation model of LS174T cells with *TP53* mutation. In a previous study, *TP53* mutation in colorectal cancer cells suppressed the function of P53 and induced more malignant phenotypes, mimicking the process of adenoma–carcinoma sequence [7]. In addition, apoptosis in UC model organoids induced by chronic inflammation was also suppressed by *TP53* mutation [6]. In this study, apoptosis induced by chronic inflammation was suppressed in *TP53*-mutated cancer cells. *TP53*-mutated cancer cells showed higher proliferation than *TP53*WT cancer cells under chronic inflammation. These results suggest that the change of malignant phenotypes in LS174T cells induced by chronic inflammation was mediated by P53. Invasiveness, which is promoted by chronic inflammation, was further enhanced in *TP53* mutated cells. These results suggest that *TP53* mutation is important for acquiring higher malignant phenotypes, even in sporadic colorectal cancer cells under chronic inflammation.

In our previous study, changes in phenotype, gene expression and histological characteristics in the UC-mimicking organoid model were found to be irrecoverable after the cessation of chronic inflammation [6]. In this study, however, the change in NF- κ B signal and malignant phenotypes of colorectal cancer cells was almost completely recovered after the removal of inflammatory stimuli, although some genes related to chronic inflammation (*QKI* and *FGF20*) were irrecoverably induced. These results suggest that cancer cells have higher plasticity than normal IECs and that sporadic adenocarcinoma cells do not acquire higher malignant phenotypes due to exposure to chronic inflammation.

Some limitations of our study should be considered while interpreting the results. First, we established a chronic inflammation model

from only a single colorectal cancer cell line (LS174T cells). Some of the data in this study were reinforced by our UC model [6] because apoptosis and the suppression of cell proliferation and sphere formation were also observed in UC model organoids [6]. However, more biological replicates should be performed to confirm our results. Second, the difference in the irrecoverable changes between organoids and LS174T cells may have been affected by the culture conditions because organoids embedded with Matrigel were cultured three-dimensionally and LS174T cells were cultured on a flat surface. Recently, the organoids culture system enabled us to directly assess the difference of IECs [20, 21]. Therefore, organoids established from sporadic neoplasms in patients with UC would enable better characterisation of these tumours. Third, we often encounter technical difficulties during endoscopic resection of sporadic neoplasms in patients with UC due to fibrosis or scars. Thus, future studies should assess the influence of chronic inflammation on not only IECs but also stromal cells.

In conclusion, this study highlighted the influence of chronic inflammation on sporadic neoplasm. Although the malignant phenotypes of sporadic neoplasms were altered by chronic inflammation, cancer cells showed higher plasticity and recovered to their original state after the removal of inflammatory stimuli.

Author contributions

S.W. performed the majority of experiments and wrote the manuscript; S.H., N.K., S.K. and A.S. provided technical assistance; R.O. and M.W. supervised the experiments and K.T. supervised the overall study

and assisted with the manuscript drafting.

Declaration of competing interest

The authors declare that they have no known competing financial interests or personal relationships that could have appeared to influence the work reported in this paper.

Acknowledgments

This work was supported by scientific Research grants from the Japanese Ministry of Education, Culture, Sports, Science and Technology (KAKENHI grant numbers 17H06654, 17K19513, 18H02791, 18K19535, 19K17425, 19H01050 and 20K22867); The Research Center Network for Realization of Regenerative Medicine project from Japan Agency for Medical Research and Development (grant numbers 18bm03041h0006 and 19bm0304001h0007); and Naoki Tsuchida Research Grant. The authors would like to thank Enago (www.enago.jp) for the English language review.

Appendix A. Supplementary data

Supplementary data to this article can be found online at <https://doi.org/10.1016/j.bbrep.2021.101031>.

References

- [1] J.A. Eaden, K.R. Abrams, J.F. Mayberry, The risk of colorectal cancer in ulcerative colitis: a meta-analysis, *Gut* 48 (2001) 526–535, <https://doi.org/10.1136/gut.48.4.526>.
- [2] M. Yashiro, Molecular alterations of colorectal cancer with inflammatory bowel disease, *Dig. Dis. Sci.* 60 (2015) 2251–2263, <https://doi.org/10.1007/s10620-015-3646-4>.
- [3] A. Leslie, F.A. Carey, N.R. Pratt, R.J. Steele, The colorectal adenoma-carcinoma sequence, *Br. J. Surg.* 89 (2002) 845–860, <https://doi.org/10.1046/j.1365-2168.2002.02120.x>.
- [4] M. Mutaguchi, M. Naganuma, S. Sugimoto, T. Fukuda, K. Nanki, S. Mizuno, N. Hosoe, M. Shimoda, H. Ogata, Y. Iwao, T. Kanai, Difference in the clinical characteristic and prognosis of colitis-associated cancer and sporadic neoplasia in ulcerative colitis patients, *Dig. Liver Dis.* 51 (2019) 1257–1264, <https://doi.org/10.1016/j.dld.2019.05.003>.
- [5] L. Laine, T. Kaltenbach, A. Barkun, K.R. McQuaid, V. Subramanian, R. Soetikno, SCENIC international consensus statement on surveillance and management of dysplasia in inflammatory bowel disease, *Gastroenterology* 148 (2015) 639–651, <https://doi.org/10.1053/j.gastro.2015.01.031>, e628.
- [6] S. Watanabe, R. Nishimura, T. Shirasaki, N. Katsukura, S. Hibiya, S. Kirimura, M. Negi, R. Okamoto, Y. Matsumoto, T. Nakamura, M. Watanabe, K. Tsuchiya, Schlafen 11 is a novel target for mucosal regeneration in ulcerative colitis, *J Crohns Colitis* (2021) jjab032, <https://doi.org/10.1093/ecco-jcc/jjab032>.
- [7] S. Watanabe, K. Tsuchiya, R. Nishimura, T. Shirasaki, N. Katsukura, S. Hibiya, R. Okamoto, T. Nakamura, M. Watanabe, TP53 mutation by CRISPR system enhances the malignant potential of colon cancer, *Mol. Canc. Res.* 17 (2019) 1459–1467, <https://doi.org/10.1158/1541-7786.mcr-18-1195>.
- [8] X. Zheng, K. Tsuchiya, R. Okamoto, M. Iwasaki, Y. Kano, N. Sakamoto, T. Nakamura, M. Watanabe, Suppression of hah1 gene expression directly regulated by hes1 via notch signaling is associated with goblet cell depletion in ulcerative colitis, *Inflamm. Bowel Dis.* 17 (2011) 2251–2260, <https://doi.org/10.1002/ibd.21611>.
- [9] E. Fathi, R. Farahzadi, S. Javanmardi, I. Vietor, L-carnitine extends the telomere length of the cardiac differentiated CD117(+)-expressing stem cells, *Tissue Cell* 67 (2020) 101429, <https://doi.org/10.1016/j.tice.2020.101429>.
- [10] B. Brazvan, R. Farahzadi, S.M. Mohammadi, S. Montazer Saheb, D. Shanebandi, L. Schmed, J. Soleimani Rad, M. Darabi, H. Nozad Charoudeh, Key immune cell cytokines Affects the telomere activity of cord blood cells in vitro, *Adv. Pharmaceut. Bull.* 6 (2016) 153–161, <https://doi.org/10.15171/apb.2016.022>.
- [11] R. Farahzadi, E. Fathi, I. Vietor, Mesenchymal stem cells could be considered as a candidate for further studies in cell-based therapy of Alzheimer's disease via targeting the signaling pathways, *ACS Chem. Neurosci.* 11 (2020) 1424–1435, <https://doi.org/10.1021/acscchemneuro.0c00052>.
- [12] K. Fukushima, K. Tsuchiya, Y. Kano, N. Horita, S. Hibiya, R. Hayashi, K. Kitagaki, M. Negi, E. Itoh, T. Akashi, Y. Eishi, S. Oshima, T. Nagaishi, R. Okamoto, T. Nakamura, M. Watanabe, Atonal homolog 1 protein stabilized by tumor necrosis factor α induces high malignant potential in colon cancer cell line, *Canc. Sci.* 106 (2015) 1000–1007, <https://doi.org/10.1111/cas.12703>.
- [13] M. Aragaki, K. Tsuchiya, R. Okamoto, S. Yoshioka, T. Nakamura, N. Sakamoto, T. Kanai, M. Watanabe, Proteasomal degradation of Atoh1 by aberrant Wnt signaling maintains the undifferentiated state of colon cancer, *Biochem. Biophys. Res. Commun.* 368 (2008) 923–929, <https://doi.org/10.1016/j.bbrc.2008.02.011>.
- [14] E. Fathi, I. Vietor, Mesenchymal stem cells promote Caspase expression in Molt-4 leukemia cells via GSK-3 α / β and ERK1/2 signaling pathways as a therapeutic strategy, *Curr. Gene Ther.* 21 (2021) 81–88, <https://doi.org/10.2174/1566523220666201005111126>.
- [15] E. Fathi, R. Farahzadi, B. Valipour, Alginate/gelatin encapsulation promotes NK cells differentiation potential of bone marrow resident C-kit(+) hematopoietic stem cells, *Int. J. Biol. Macromol.* 177 (2021) 317–327, <https://doi.org/10.1016/j.ijbiomac.2021.02.131>.
- [16] S. Hibiya, K. Tsuchiya, R. Hayashi, K. Fukushima, N. Horita, S. Watanabe, T. Shirasaki, R. Nishimura, N. Kimura, T. Nishimura, N. Gotoh, S. Oshima, R. Okamoto, T. Nakamura, M. Watanabe, Long-term inflammation transforms intestinal epithelial cells of colonic organoids, *J Crohns Colitis* 11 (2017) 621–630, <https://doi.org/10.1093/ecco-jcc/jjw186>.
- [17] J.Y. Lee, M.K. Park, J.H. Park, H.J. Lee, D.H. Shin, Y. Kang, C.H. Lee, G. Kong, Loss of the polycomb protein Mel-18 enhances the epithelial-mesenchymal transition by ZEB1 and ZEB2 expression through the downregulation of miR-205 in breast cancer, *Oncogene* 33 (2014) 1325–1335, <https://doi.org/10.1038/ncr.2013.53>.
- [18] H. Solomon, N. Dinowitz, I.S. Pateras, T. Cooks, Y. Shetzer, A. Molchadsky, M. Charni, S. Rabani, G. Koifman, O. Tarcic, Z. Porat, I. Kogan-Sakin, N. Goldfinger, M. Oren, C.C. Harris, V.G. Gorgoulis, V. Rotter, Mutant p53 gain of function underlies high expression levels of colorectal cancer stem cells markers, *Oncogene* 37 (2018) 1669–1684, <https://doi.org/10.1038/s41388-017-0060-8>.
- [19] M. Dohadwala, G. Wang, E. Heinrich, J. Luo, O. Lau, H. Shih, Q. Munaim, G. Lee, L. Hong, C. Lai, E. Abemayor, M.C. Fishbein, D.A. Elashoff, S.M. Dubinett, M.A. St John, The role of ZEB1 in the inflammation-induced promotion of EMT in HNSCC, *Otolaryngol. Head Neck Surg.* 142 (2010) 753–759, <https://doi.org/10.1016/j.otohns.2010.01.034>.
- [20] E. d'Aldebert, M. Quaranta, M. Sébert, D. Bonnet, S. Kirzin, G. Portier, J.P. Duffas, S. Chabot, P. Lluet, S. Allart, A. Ferrand, L. Alric, C. Racaud-Sultan, E. Mas, C. Deraison, N. Vergnolle, Characterization of human colon organoids from inflammatory bowel disease patients, *Front Cell Dev Biol* 8 (2020) 363, <https://doi.org/10.3389/fcell.2020.00363>.
- [21] J. Krafczy, M. Zilbauer, Intestinal epithelial organoids as tools to study epigenetics in gut health and disease, *Stem Cell. Int.* 2019 (2019) 7242415, <https://doi.org/10.1155/2019/7242415>.